

# Synthesis, characterization and thermal behaviour of solid-state compounds of folates with some bivalent transition metals ions

P. R. Dametto · B. Ambrozini · F. J. Caires ·  
V. P. Franzini · M. Ionashiro

Received: 20 March 2013 / Accepted: 28 May 2013 / Published online: 22 June 2013  
© Akadémiai Kiadó, Budapest, Hungary 2013

**Abstract** Solid-state M–L compounds, where M stands for bivalent Mn, Co, Ni, Cu and Zn and L is folate ( $C_{19}H_{17}N_7O_6$ ), have been synthesized. Simultaneous thermogravimetry and differential scanning calorimetry (TG–DSC), X-ray powder diffractometry, infrared spectroscopy (FTIR), TG–DSC coupled to FTIR, elemental analysis and high-resolution continuum source flame atomic absorption spectrometry technique (HR-CS FAAS) were used to characterize and to study the thermal behaviour of these compounds. The results provided information concerning the composition, dehydration, thermal stability and thermal decomposition.

**Keywords** Bivalent transition metals · Folate · Characterization · Thermal behavior

## Introduction

Folic acid as reported in the figure, *N*-(4-((2-amino-4-oxo-1,4-dihydropteridin-6-yl)methyl)amino)benzoyl)-L-glutamic acid is from a group of vitamins called water soluble vitamins, which contain B-group vitamins and the other group [1]. Folic acid is necessary to healthy function of a variety of bodily processes. Folic acid and its derivatives are widespread among the nature. Folic acid is a specific growth factor for certain microorganisms; however, in animals the intestinal bacteria provides small amounts needed for growth. It acts as co-enzyme in the normal DNA

synthesis, and also functions as part of the co-enzyme system in amino acid and nucleoprotein synthesis [2–4]. The structural diversity found in metal folate complexes can be attributed to the versatile behaviour of the folate anion, which may act as bidentate, bridging bidentate or as a monodentate ligand [2, 3, 5, 6].

A survey of the literature shows that the thermal studies involving folic acid or its compounds with metal ions is lacking. The articles published are concerned with thermal stability of folic acid or folates in the solid-state [2, 3]; synthesis, spectroscopic, and thermal characterization of some transition metal complexes of folic acid [5]; and processes to identify the degradation mechanism of a solid which appears to undergo a complex reaction: folic acid [6].

In this article, the objective of the present research was to prepare solid-state compounds from some bivalent transition metals with folate and to investigate them by means of high-resolution continuum source flame atomic absorption spectrometry technique (HR-CS FAAS), elemental analysis, X-ray powder diffractometry, infrared spectroscopy (FTIR), simultaneous thermogravimetry and differential scanning calorimetry (TG–DSC).

## Experimental

The folic acid ( $C_{19}H_{19}N_7O_6$ ) with 99 % purity was obtained from Aldrich. Aqueous solution of sodium folate  $0.10 \text{ mol L}^{-1}$  was prepared by neutralization of folic acid in aqueous solution with  $0.10 \text{ mol L}^{-1}$  sodium hydroxide solution. Aqueous solutions of bivalent metal ions  $0.10 \text{ mol L}^{-1}$  were prepared by dissolving the corresponding chloride (Mn(II), Co(II), Ni(II), Zn(II)) or sulphate (Cu(II)).

P. R. Dametto (✉) · B. Ambrozini · F. J. Caires ·  
V. P. Franzini · M. Ionashiro  
Instituto de Química, UNESP, C. P. 355, Araraquara,  
SP CEP 14801-970, Brazil  
e-mail: pdametto@gmail.com

The solid-state compounds were prepared by adding slowly, with continuous stirring, the solution of the ligand (100.0 mL, 0.10 mol L<sup>-1</sup>) to the hot solution of the respective metal ions solutions (50.0 mL, 0.10 mol L<sup>-1</sup>), until total precipitation of the metal ions. The precipitates were washed with distilled water, until elimination of chloride or sulphate ions (qualitative test with AgNO<sub>3</sub>/HNO<sub>3</sub> solution for chloride or BaCl<sub>2</sub> solution for sulphate), filtered through and dried on Whatman no 42 filter paper, and kept in a desiccator over anhydrous calcium chloride.

In the solid-state compounds hydration water, ligand and metal ion content were determined from TG curves. The metal ions were also determined using a Perkin Elmer AAnalyst 100 Flame Atomic Absorption Spectrometer (Shelton, CT, USA) equipped with hollow-cathode lamps as radiation sources for Mn (slit = 0.2 nm;  $\lambda$  = 279.5 nm), Co (slit = 0.2 nm;  $\lambda$  = 240.7 nm), Ni (slit = 0.2 nm;  $\lambda$  = 232.0 nm), Cu (slit = 0.7 nm;  $\lambda$  = 324.8 nm) and Zn (slit = 0.7 nm;  $\lambda$  = 213.9 nm) determination. An oxidizing air/acetylene flame (Air Liquide, Sertãozinho, Brazil) was used for analyte atomization. In instrument an aspiration rate of about 5 mL min<sup>-1</sup> was used. Measurements of each analyte were carried out in triplicate. A heating block (Tecnal, TE 015-150, Piracicaba, Brazil) was used to evaporate water samples.

The solutions were made using high purity water obtained with a Millipore Rios 5<sup>TM</sup> reverse osmosis and a Millipore Milli-Q Academic TM system (resistivity 18.2 M $\Omega$  cm) was used throughout the study. For Mn, Co, Ni, Cu and Zn analysis using the AAnalyst 100 spectrometer, analytical solutions (0.25–2.0 mg L<sup>-1</sup> Mn; 0.5–3.0 mg L<sup>-1</sup> Co; 0.1–1.0 mg L<sup>-1</sup> Ni; 2.5–10 mg L<sup>-1</sup> Cu e 0.1–1.0 mg L<sup>-1</sup> Zn) were prepared by appropriate dilution of the 1000.0 mg L<sup>-1</sup> stock standard solutions (Normex TM, Carlo Erba, Italy). All analytical solutions and samples were acidified to 1 % v/v HNO<sub>3</sub> from a 70 % v/v HNO<sub>3</sub> solution (Spectrum, New Brunswick, NJ, USA) to avoid hydrolysis.

Carbon and hydrogen contents were determined by microanalytical procedures, with a CHN Elemental Analyser from Perkin Elmer, model 2400.

X-ray powder patterns were obtained by using a SIEMENS D-5000 X-ray Diffractometer employing Cu K $\alpha$  radiation ( $\lambda$  = 1.541 Å) and setting of 40 kV and 20 mA.

The attenuate total reflectance infrared spectra for sodium folate and for its metal-ion compounds were run on a Nicolet iS10 FT-IR Spectrophotometer, using an ATR accessory with Ge window. The FTIR spectra were recorded with 32 scans per spectrum at resolution of 4 cm<sup>-1</sup>.

Simultaneous TG–DSC curves were obtained by using a TGA–DSC 1 Stare system, from Mettler Toledo. The purge gas was an air flow of 50 mL min<sup>-1</sup> and a heating rate of 10 K min<sup>-1</sup> was adopted, with samples weighing about 3.7 mg. Alumina crucibles were used for recording the TG–DSC curves.

The TG–FTIR experiments were performed using a Thermogravimetric Analyzer Mettler TG–DSC, coupled to a Nicolet iS10 FTIR Spectrometer equipped with an IR gas cell. The transfer line consists of a stainless steel tube of 120 cm in length (2 mm in inner diameter) heated at a constant temperature of 523 K. FTIR measurements were carried out with a DTGS detector in a specifically developed gas cell, heated at a constant temperature of 498 K. The interferometer and the gas cell compartments were purged with high purified N<sub>2</sub>. The FTIR spectra were recorded with 16 scans per spectrum at resolution of 4 cm<sup>-1</sup>.

## Results and discussion

The analytical and thermoanalytical (TG) data for the synthesized compounds are shown in Table 1. These results establish the stoichiometry of these compounds, which are in agreement with the general formula, [ML] $\cdot n$ H<sub>2</sub>O, where M represents Mn(II), Co(II), Ni(II), Cu(II) e Zn(II), L is folate and  $n$  = 3.5 (Mn), 4.0 (Co), 3.5 (Ni), 3.5 (Cu) e 3.0 (Zn).

The X-ray diffraction powder patterns (Fig. 1) show that all the compounds have crystalline structure and form an isomorphous group. The crystallinity of these compounds

**Table 1** Analytical data for [ML] $\cdot n$ H<sub>2</sub>O

Compounds	Water/%		Ligand lost/%		Metal/%			Carbon/%		Hydrogen/%		Nitrogen/%		Residue
	Calcd.	TG	Calcd.	TG	Calcd.	TG	HR-CS FAAS	Calcd.	E.A.	Calcd.	E.A.	Calcd.	E.A.	
[MnL] $\cdot 3.5$ H <sub>2</sub> O	11.32	10.74	74.52	74.47	9.86	10.29	9.67	40.94	40.91	4.35	4.32	17.59	17.58	MnO
[CoL] $\cdot 4$ H <sub>2</sub> O	12.64	12.33	74.18	75.30	10.33	9.73	9.82	40.01	40.61	4.43	4.47	17.19	17.45	CoO
[NiL] $\cdot 3.5$ H <sub>2</sub> O	11.24	11.56	75.49	74.33	10.46	11.06	10.33	40.66	40.04	4.32	4.28	17.48	17.21	NiO
[CuL] $\cdot 3.5$ H <sub>2</sub> O	11.14	11.73	74.90	75.09	11.23	10.53	11.07	40.32	40.42	4.28	4.32	17.33	17.37	CuO
[ZnL] $\cdot 3$ H <sub>2</sub> O	9.67	9.99	75.82	75.06	11.70	12.00	11.48	40.83	40.43	4.16	4.14	17.55	17.46	ZnO

M Mn(II), Co(II), Ni(II), Cu(II), Zn(II); L folate

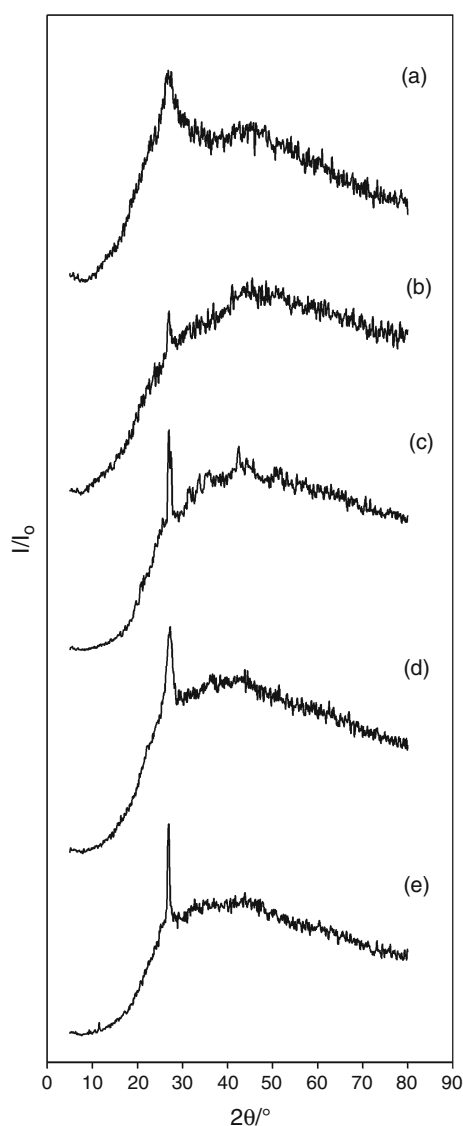


**Fig. 1** X-ray powder diffraction patterns of the compounds: (a) [MnL]·3.5H<sub>2</sub>O; (b) [CoL]·4H<sub>2</sub>O; (c) [NiL]·3.5H<sub>2</sub>O; (d) [CuL]·3.5H<sub>2</sub>O; (e) [ZnL]·3H<sub>2</sub>O. L folate

follow the order: Zn > Cu > Ni > Co > Mn. The difference in the crystallinity of these compounds must be probably due to the solubility of each compound and the velocity of the evaporation, which was not controlled.

Infrared spectroscopic data on sodium folate (Na<sub>2</sub>L) and its compounds with the metal ions considered in this study are shown in Table 2. The investigation was focused mainly within the 1700–1400 cm<sup>-1</sup> range because this region is potentially most informative in attempting to assign coordination sites. In the Na<sub>2</sub>L, strong bands located at 1564 and 1392 cm<sup>-1</sup> are attributed to anti-symmetrical ( $\nu_{as}$ ) and symmetrical ( $\nu_s$ ) frequencies of the carboxylate groups, respectively [7, 8]. For the synthesized compounds the band assigned to the anti-symmetrical stretching

**Table 2** Spectroscopic data for sodium folate and compounds with bivalents transition metals

Compounds	$\nu_{as}(\text{COO}^-)/\text{cm}^{-1}$	$\nu_s(\text{COO}^-)/\text{cm}^{-1}$	$\Delta\nu(\nu_{as} - \nu_s)/\text{cm}^{-1}$
Na <sub>2</sub> L	1564 <sub>s</sub>	1392 <sub>s</sub>	172
[MnL]·3.5H <sub>2</sub> O	1527 <sub>s</sub>	1410 <sub>s</sub>	117
[CoL]·4H <sub>2</sub> O	1513 <sub>s</sub>	1407 <sub>s</sub>	106
[NiL]·3.5H <sub>2</sub> O	1516 <sub>s</sub>	1408 <sub>s</sub>	108
[CuL]·3.5H <sub>2</sub> O	1510 <sub>s</sub>	1402 <sub>s</sub>	108
[ZnL]·3H <sub>2</sub> O	1511 <sub>s</sub>	1407 <sub>s</sub>	104

$\nu_s(\text{COO}^-)$  and  $\nu_{as}(\text{COO}^-)$  = symmetrical and anti-symmetrical vibrations of the COO<sup>-</sup> structure

*s* Strong, *L* folate

carboxylate frequencies are shifted to lower values and the symmetrical ones to higher, relative to the corresponding frequencies in C<sub>19</sub>H<sub>17</sub>N<sub>7</sub>O<sub>6</sub>, suggesting the participation of this group in the coordination. The values of  $\Delta\nu$  ( $\nu_{as} \text{COO}^- - \nu_s \text{COO}^-$ , carboxylate vibrations) for the synthesized compounds are smaller than those ones calculated for the sodium salt (Table 2), suggesting that the coordination is carried out through the carboxylate group of the folate in a chelating and/or bridging mode [9].

Simultaneous TG–DSC curves of the compounds are shown in Fig. 2. The TG curves show mass losses in three or four steps, corresponding to endothermic peaks attributed to dehydration or reduction reaction and exothermic peaks due to oxidation of organic matter and/or gaseous products evolved during the thermal decomposition.

After dehydration the mass losses observed are due to the thermal decomposition of the anhydrous compounds, which occur in consecutive and/or overlapping steps with partial losses characteristic for each compound.

The thermal stability of the compounds (I), shown by TG–DSC curves (Fig. 2) depends on the nature of the metal ion, and follow the order:

(I) Zn > Cu > Mn > Co > Ni

The TG–DSC curves also show that the formation of stable anhydrous compounds is observed only for zinc compounds, while for manganese, cobalt, nickel and copper ones the thermal decomposition occurs immediately after the dehydration. The thermal behavior of the compounds will be discussed individually.

#### Manganese compound

The simultaneous TG–DSC curves are shown in Fig. 2a. The first mass loss observed between 321 and 401 K (TG), corresponding to an endothermic peak at 368 K (DSC) is due to dehydration with loss of 3.5H<sub>2</sub>O (calcd. = 11.32 %, TG = 10.74 %). The thermal decomposition of the anhydrous

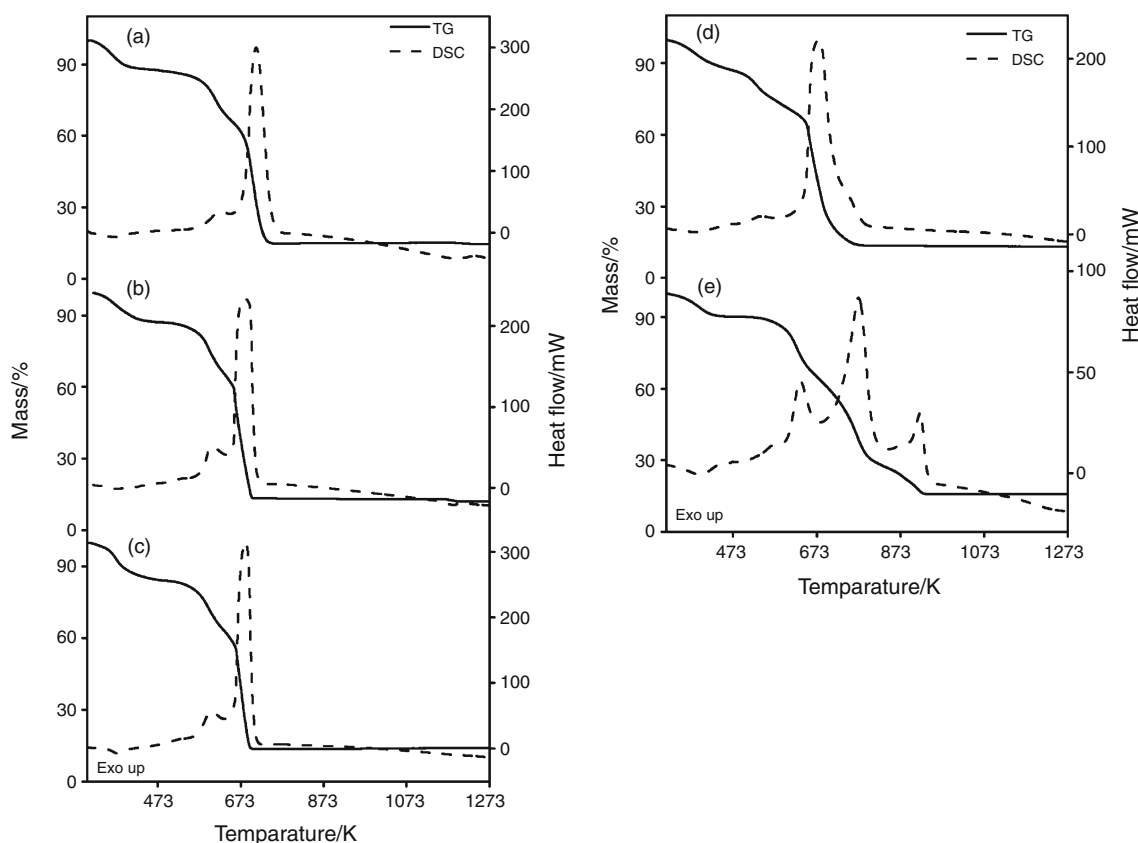


**Fig. 2** TG–DSC curves of: (a)  $[\text{MnL}] \cdot 3.5\text{H}_2\text{O}$  ( $m = 3.735$  mg); (b)  $[\text{CoL}] \cdot 4\text{H}_2\text{O}$  ( $m = 3.719$  mg); (c)  $[\text{NiL}] \cdot 3.5\text{H}_2\text{O}$  ( $m = 3.755$  mg); (d)  $[\text{CuL}] \cdot 3.5\text{H}_2\text{O}$  ( $m = 3.735$  mg); (e)  $[\text{ZnL}] \cdot 3\text{H}_2\text{O}$  ( $m = 3.160$  mg).  $L = \text{folate}$

compounds occurs in two consecutive and/or overlapping steps, between 401 and 753 K with loss of 74.47 %, corresponding to the exothermic peak at 623 K (DSC) and 710 K (DSC), which are attributed to the oxidation of the organic matter. The total mass loss up to 753 K is in agreement with the formation of  $\text{Mn}_3\text{O}_4$ , which was confirmed by X-ray powder diffractometry. It was observed an endothermic event in 1,190 K that is assigned to the reduction of  $\text{Mn}_3\text{O}_4$  to  $\text{MnO}$  in agreement with the literature [10, 11].

#### Cobalt compound

The simultaneous TG–DSC curves are shown in Fig. 2b. The first mass loss that occurs between 311 and 448 K (TG), corresponding to endothermic event at 373 K (DSC) is due to dehydration with loss of  $4\text{H}_2\text{O}$  (calcd. = 12.64 %, TG = 12.33 %). The thermal decomposition of the anhydrous compound occurs in two consecutive and/or overlapping steps between 463 and 703 K with loss of 74.33 %, corresponding to exothermic peak at 607 and 681 K (DSC), attributed to oxidation of the organic matter. The total mass loss up to 708 K is in agreement with the formation of  $\text{Co}_3\text{O}_4$  (calcd. = 85.41 %, TG = 86.66 %). The last mass loss that occurs between 1168 and 1193 K,

corresponding to the endothermic peak at 1,178 K (DSC) is attributed to reduction of  $\text{Co}_3\text{O}_4$  to  $\text{CoO}$  (calcd. = 1.41 %, TG = 0.9679 %), in agreement with the literature [11–13].

#### Nickel compound

The simultaneous TG–DSC curves are shown in Fig. 2c. The mass loss that occurs between 313 and 403 K, corresponding to endothermic peak at 373 K (DSC), is due to dehydration with loss of  $3.5\text{H}_2\text{O}$  (calcd. = 11.24 %, TG = 11.56 %). After the dehydration the thermal decomposition between 403 and 703 K occurs in two consecutive and/or overlapping steps, where the mass loss begins with a slow process, followed by a fast one, with loss of 74.33 %. This mass loss corresponds to exothermic peaks at 602 and 685 K (DSC) attributed to oxidation of the organic matter. The total mass loss up to 703 K is in agreement with the formation of  $\text{NiO}$  as final residue (calcd. = 86.73 %, TG = 85.93 %).

#### Copper compound

The simultaneous TG–DSC curves are shown in Fig. 2d. The mass loss observed between 308 and 451 K (TG), corresponding to endothermic event at 374 K (DSC) is due to

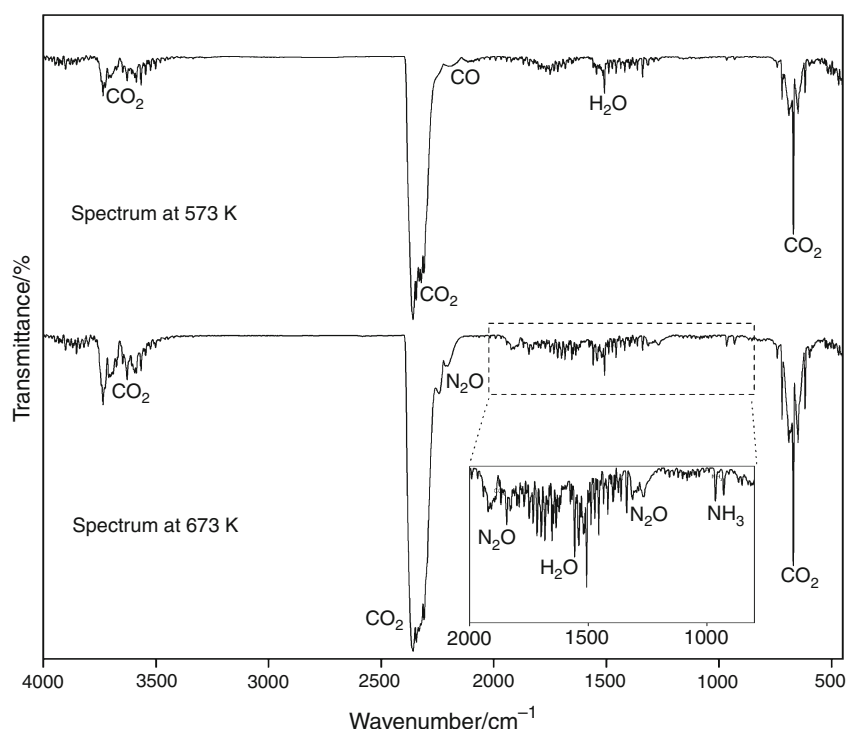


**Fig. 3** IR spectra of gaseous products evolved during the decomposition of the cobalt folate

dehydration with loss of  $3.5\text{H}_2\text{O}$  (calcd. = 11.14 %, TG = 11.73 %). After the dehydration the thermal decomposition begins through a slow process, followed by a fast one between 451 and 883 K with loss of 75.09 % corresponding to exothermic peak at 544 K (DSC) and 678 K (DSC) attributed to oxidation of organic matter. The mass loss up to 883 K is in agreement with the formation of the CuO as residue (calcd. = 86.04 %, TG = 86.82 %).

#### Zinc compound

The TG–DSC curves are shown in Fig. 2e. The mass loss observed between 313 and 463 K (TG), corresponding to the endothermic peak at 392 K (DSC) is due to dehydration with loss of  $3\text{H}_2\text{O}$  (calcd. = 9.67 %, TG = 9.99 %). The anhydrous compound is stable up to 514 K and above this temperature the thermal decomposition occurs between 514 and 918 K with loss of 75.06 %, corresponding to exothermic peaks at 629, 759, 866, 891 K (DSC) attributed to oxidation of organic matter. The total mass loss up to 918 K is in agreement with the formation of ZnO as final residue (calcd. = 75.82 %, TG = 75.06 %).

The gaseous products evolved during the thermal decomposition of the transition metal ion compounds studied in this study were monitored by FTIR, and it has water, carbon dioxide, carbon monoxide, nitrous oxide and ammonia as main products due to the decarboxylation and

oxidation of organic matter. The IR spectra of the gaseous products evolved during the thermal decomposition cobalt folate, as representative of all the compounds are shown in Fig. 3.

#### Conclusions

From TG, flame atomic absorption spectrometry technique and elemental analysis results, a general formula could be established for the synthesized compounds.

The X-ray powder patterns showed that all the compounds have a tendency to crystalline, with evidence for formation of isomorphous series.

The infrared spectroscopic data suggest that  $\text{C}_{19}\text{H}_{17}\text{N}_7\text{O}_6$  acts as a chelating and/or bridging bidentate ligand to the metal ions through the carboxylate group.

The simultaneous TG–DSC curves provided previously unreported information about the thermal stability and thermal decomposition of these compounds in dynamic air atmosphere.

The monitoring of evolved gases during the heating of cobalt folate showed water, carbon dioxide, carbon monoxide, nitrous oxide and ammonia as main products due to the decarboxylation and oxidation of organic matter.

**Acknowledgements** The authors thank FAPESP, CNPq and CAPES Foundations (Brazil) for financial support.

## References

1. Hamed E, Attia MS, Bassiouny K. Synthesis, spectroscopic and thermal characterization of copper(II) and iron(III) complexes of folic acid and their absorption efficiency in the blood. *Bioinorg Chem Appl* 2009. doi:10.1155/2009/979680.
2. Dametto PR, Caires FJ, Ambrozini B, Ionashiro M. Synthesis, characterization and thermal behaviour of light trivalent lanthanides folates on solid state. *J Therm Anal Calorim*. 2011;105:831–6.
3. Vora A, Riga A, Dollimore D, Alexander K. Thermal stability of folic acid in the solid-state. *J Therm Anal Calorim*. 2004;75:709–17.
4. Mehrotra RC, Singh A. Recent trends in metal alkoxide chemistry. *Prog Inorg Chem*. 1997;46:239–454.
5. Abd El-Wahed MG, Refat MS, El-Megharbel SM. Synthesis, spectroscopic and thermal characterization of some transition metal complexes of folic acid. *Spectrochim Acta A*. 2008;70:916–22.
6. Vora A, Riga A, Alexander K. Processes to identify the degradation mechanism of a solid which appears to undergo a complex reaction: folic acid. *Instrum Sci Technol*. 2002;30:193–203.
7. Sócrates G. *Infrared characteristic group frequencies*. 2nd ed. New York: Wiley; 1994.
8. Silverstein RM, Webster FX. *Spectrometric identification of organic compounds*. 6th ed. New York: Wiley; 1998.
9. Deacon GB, Phillips RJ. Relationships between the carbon-oxygen stretching frequencies of carboxylate complexes and the type of carboxylate coordination. *Coord Chem Rev*. 1980;33:227–50.
10. Biernacki L, Pokrzywnicki S. The thermal decomposition of manganese carbonate. *J Therm Anal Calorim*. 1999;55:227–32.
11. Caires FJ, Lima LS, Carvalho CT, Giaggio RJ, Ionashiro M. Thermal behaviour of malonic acid, sodium malonate and its compounds with some bivalent transition metal ions. *Thermochim Acta*. 2010;497:35–40.
12. El-Shobaky GA, Ahmad AS, Al Noaim AN, El-Shobaky HG. Thermal decomposition of basic cobalt and copper carbonates. Thermal stability of the produced oxides as influenced by gamma-irradiation. *J Therm Anal*. 1996;46:1801–8.
13. Bannach G, Siqueira AB, Ionashiro EY, Rodrigues EC, Ionashiro M. Solid-state compounds of 2-chlorobenzylidenepyruvate with some bivalent metal ions: synthesis, characterization and thermal behaviour. *J Therm Anal Calorim*. 2007;90:873–9.